crystals

MDPI

Article

Low Temperature and High-Pressure Study of Bending L-Leucinium Hydrogen Maleate Crystals

Kseniya D. Skakunova [1,2] and Denis A. Rychkov [1,2,*]

[1] Institute of Solid State Chemistry and Mechanochemistry, Siberian Branch of Russian Academy of Sciences, 630090 Novosibirsk, Russia; skakunova.kseniya@mail.ru
[2] Laboratory of Physicochemical Fundamentals of Pharmaceutical Materials, Faculty of Natural Sciences, Novosibirsk State University, 630090 Novosibirsk, Russia
* Correspondence: rychkov.dennis@gmail.com; Tel.: +7-383-233-24-10 (ext. 1130)

Abstract: The polymorphism of molecular crystals is a well-known phenomenon, resulting in modifications of physicochemical properties of solid phases. Low temperatures and high pressures are widely used to find phase transitions and quench new solid forms. In this study, L-Leucinium hydrogen maleate (LLHM), the first molecular crystal that preserves its anomalous plasticity at cryogenic temperatures, is studied at extreme conditions using Raman spectroscopy and optical microscopy. LLHM was cooled down to 11 K without any phase transition, while high pressure impact leads to perceptible changes in crystal structure in the interval of 0.0–1.35 GPa using pentane-isopentane media. Surprisingly, pressure transmitting media (PTM) play a significant role in the behavior of the LLHM system at extreme conditions—we did not find any phase change up to 3.05 GPa using paraffin as PTM. A phase transition of LLHM to amorphous form or solid–solid phase transition(s) that results in crystal fracture is reported at high pressures. LLHM stability at low temperatures suggests an alluring idea to prove LLHM preserves plasticity below 77 K.

Keywords: plastic crystals; Raman spectroscopy; low temperature; high-pressure; L-Leucinium hydrogen maleate; plasticity; bending crystal

Citation: Skakunova, K.D.; Rychkov, D.A. Low Temperature and High-Pressure Study of Bending L-Leucinium Hydrogen Maleate Crystals. *Crystals* **2021**, *11*, 1575. https://doi.org/10.3390/cryst11121575

Academic Editors: Ulrich Prahl, Sergey Guk and Faisal Qayyum

Received: 23 November 2021
Accepted: 14 December 2021
Published: 16 December 2021
Corrected: 21 April 2022

1. Introduction

Studying molecular crystals and their phase transitions is of great importance for many scientific fields such as crystallography [1,2], thermodynamics [3,4], computational [5–7] and solid state chemistry [8–10], etc. Solid forms of many organic molecules are being developed, studied, and produced in the pharmaceutical industry [11–15] and in arising subfields of materials science [16–18]. The last one, among others, focuses the attention on the mechanical properties of molecular crystals [19–25] and metal-organic complexes [26–28]. Several dozens of organic crystals show anomalous plasticity and elasticity at ambient and extreme conditions under mechanical stress [29–33]. L-Leucinium hydrogen maleate (LLHM) is a unique example of organic crystals that preserves plasticity at a cryogenic temperature [34]. This phenomenon was studied and explained recently using a mainly crystallographic approach [34,35].

One of the methods to understand the nature of an important property of molecular crystal is to apply significant outside impact—low temperature, hydrostatic pressure, mechanochemical stress, etc. [36–39]. These methods help to follow the behavior of the systems at changing environments at macroscopic (thermodynamics) and microscopic (molecular contacts) levels, depending on the availability of experimental and theoretical techniques [40–47]. Moreover, low temperatures and high pressures often trigger phase transitions, resulting in new solid forms, including polymorphs. The application of extreme conditions is a powerful tool to find and sometimes stabilize new forms of organic molecules.

Thus, studies of new forms of molecular crystals using extreme conditions [11,37,48] as well as a search of new bending crystals [30,49,50] are of great interest for modern science. Nevertheless, the interrelation of these two areas is just an emerging field. There are very few works that search for new forms of plastic crystals at high pressures or low temperatures [34,35,51]. To fulfill this gap, in this work we applied low temperatures and high pressures to crystals of LLHM, chasing new forms of these bending crystals. In this work we continue examination of the LLHM system at different conditions, reporting experimental behavior of this crystal at extreme conditions.

L-Leucinium hydrogen maleate crystals were grown for the first time by Arkhipov et al. [52] as an individual system in a series of amino acid maleates. Providing single crystal X-ray diffraction (SCXRD) experiments, the plasticity of LLHM was noted and formulated as "interesting mechanical behavior: mechanical action on crystals of (LLHM) results in elastic, and then plastic bending". Further, a detailed study showed that crystals preserve their plasticity at temperatures down to 77 K. It was proven using video and photo recording of the bending process [34]. Using SCXRD, authors showed that no significant changes in crystal structure of LLHM occurred during the cooling down to 100 K, preserving the layered structure [34]. The system behavior on bending was also investigated using optical and scanning electron microscopy, as well as SCXRD [35]. Scrupulous analysis of crystal structure allows authors to provide a simple model for bending LLHM crystals—layers of L-Leucinium cations and maleic acid anions connected via H-bonds (forming *bc* planes) were stacked over *a* direction (interacting with weak VdW interactions). This results in the possible slipping of layers along b direction (Figure 1).

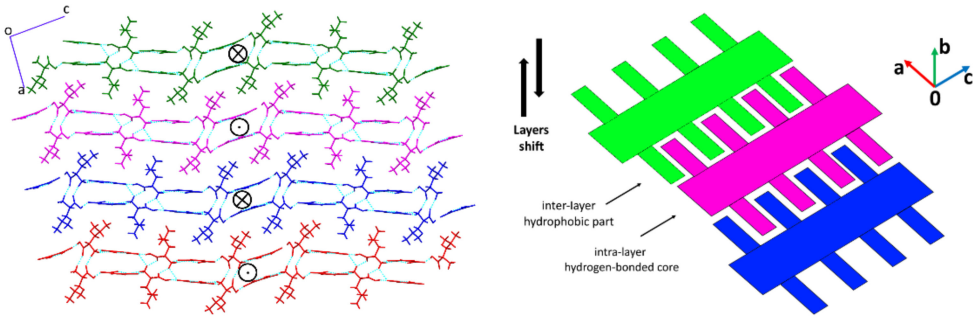

Figure 1. Crystallographic (**left**) and schematic (**right**) representation of the layered structure of LLHM, showing layers that shift resulting in plasticity under mechanical stress (adapted from [34,35]). Layers' shifts are marked with an arrow sign depending on the direction of displacement.

Nevertheless, no experiments below 100 K and high pressures were provided before, leaving an opportunity for a combined study of possible phase transitions at extreme conditions using powerful methods of XRD and Raman spectroscopy.

2. Materials and Methods

2.1. Crystal Growth

Crystals of LLHM were obtained by slow evaporation of an equimolar aqueous solution of L-leucine and maleic acid using the 'sitting-drop' approach [53] as described in previous work [34]. L-leucine (>98%, HPLC) and maleic acid (>99%, HPLC) were purchased from Sigma-Aldrich (St. Louis, MO, USA) and used without further purification. The crystallization procedure leads to 'hedgehog' polycrystalline material as presented in [35]. This bulk material was used to find and cut single crystals for low-temperature and high-pressure experiments. Crystals were operated with care at every stage of isolation and setting to the diamond anvil cell (DAC) to avoid accidental bending.

2.2. High-Pressure Generation and Measurement

Hydrostatic pressure was generated in diamond-anvil cells (DAC) of 'Almax–Boehler' type without beryllium backing plates [54] with natural diamonds suitable both for X-ray

diffraction and for Raman experiments. Paraffin (ROTH GmbH, Karlsruhe, Germany, hydrostatic limit ~3 GPa) and a 1:1 stoichiometric pentane–isopentane mixture (PIP) (hydrostatic limit 7 GPa) were used as a pressure-transmitting medium (PTM) in two separate experiments [55]. A special chamber was used to facilitate the DAC loading [56]. Pressure measurement was done with a precision of 0.05 GPa using the ruby fluorescence method [57,58].

2.3. Optical Microscopy

Optical microscopy was provided using the OLYMPUS BX41 microscope (Olympus, Tokyo, Japan) with a MPlan N 10×/0.25 FN22 objective. Euromex fiber optic light source EK-1 was used for illumination.

2.4. Single-Crystal X-ray Diffraction (SCXRD)

Data were collected using an Oxford Diffraction Gemini R Ultra X-ray diffractometer (Crawley, Australia) with a CCD area detector and Mo Kα radiation. The quality of data was not high enough to refine the atomic coordinates or determine unit cell parameters, mainly because of the DAC usage. It was mentioned before that the diffraction of LLHM crystals is not very high for accessible laboratory instruments either. [34]

2.5. Raman Spectroscopy

Raman experiments were performed for low-temperature and high-pressure samples. Raman spectra were recorded using a LabRam HR 300 spectrometer from HORIBA Jobin Yvon (Edison, NJ, USA) with a CCD detector. For spectral excitation, a 488 nm line of an Ar^+ laser was used with a beam size of ~1 μm at the surface of the sample and a power of ~8 mW. All data were collected using a Raman microscope in backscattering geometry. The spectral resolution was ~2 cm^{-1} providing seven scans 30 s each for every spectrum.

Raman spectra of LLHM were recorded in the temperature range of 300–11 K during cooling without repeating on heating.

Two distinct experiments were performed for samples at high pressures. Raman spectra for LLHM in PIP were recorded at pressures of 1.35, 2.03, 2.48, 3.06, 3.63, 4.05, 4.48, 5.03, 5.50, and 6.15 GPa on loading and 3.05, 1.82, 1.15, 0.41, and 0 GPa on pressure release. Spectra for LLHM in Paraffin were recorded at pressures of 0, 0.38, 2.55, and 2.90 GPa.

2.6. Computational Methods

Gas-phase calculations of vibrational spectra (both IR and Raman) were done for L-leucine cation, Maleic acid anion, and LLHM dimer to provide a more reasonable assignment of experimental modes. Ions of L-Leucine, maleic acid, and their dimer were extracted from the LLHM crystal structure from [34] and were further freely optimized at B3LYP/6-311+G(d,p) level of theory, providing vibrational calculations subsequently. None of the atoms or groups were fixed for gas-phase optimization, making possible the ion formation of L-Leucine and Maleic acid in the gas phase calculations. Gaussian09 package was used for all calculations [59]

Solid state calculations, as suggested in literature, were attempted to perform for the simulation of high-pressure behavior [3,7,46] and the vibrational band assignment. Nevertheless, even the usage of supercomputers (80 cpu, 384 Gb RAM, max time for task without interruption—240 h) did not allow for the performance of such calculations in reasonable time, providing the 'simple' optimization of one full unit cell in several months. Thus, only gas-phase calculations were used for this work.

3. Results

Crystals of LLHM were grown as described in the' Section 2. One crystal was used for the low temperature experiment, and another two were used in high pressure experiments in PIP and paraffin PTM. All crystals were selected using optical polarized microscopy.

3.1. Room Temperature Raman Spectra and Vibrational Mode Assignment

The crystal structure of LLHM contains six molecules in the asymmetric unit cell, resulting in 24 molecules in the full unit cell (Figure 2). Multiple H-bonds are located in directions not coinciding with cell axes or crystal faces, which limits the utility of polarized Raman spectroscopy.

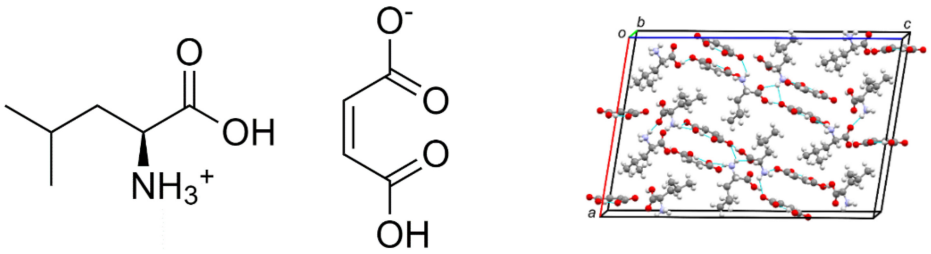

Figure 2. Molecular (**left**) and crystal structure fragment of LLHM at 298 K (**right**), showing 12 molecules of L-leucine and maleic acid each in the unit cell (CCDC# 1889564). Hydrogen bonds are shown by dashed lines.

The complicated structure of LLHM significantly constrains precise band assignment in Raman spectra. Nevertheless, literature data and calculated gas-phase vibrational spectra of L-Leucine and maleic acid ions and their dimer helps to assign main band regions of obtained experimental spectra (Figure 3) [60–66]. All literature data except ref. [67], which contains multiple inaccuracies, confirm the suggested band assignment.

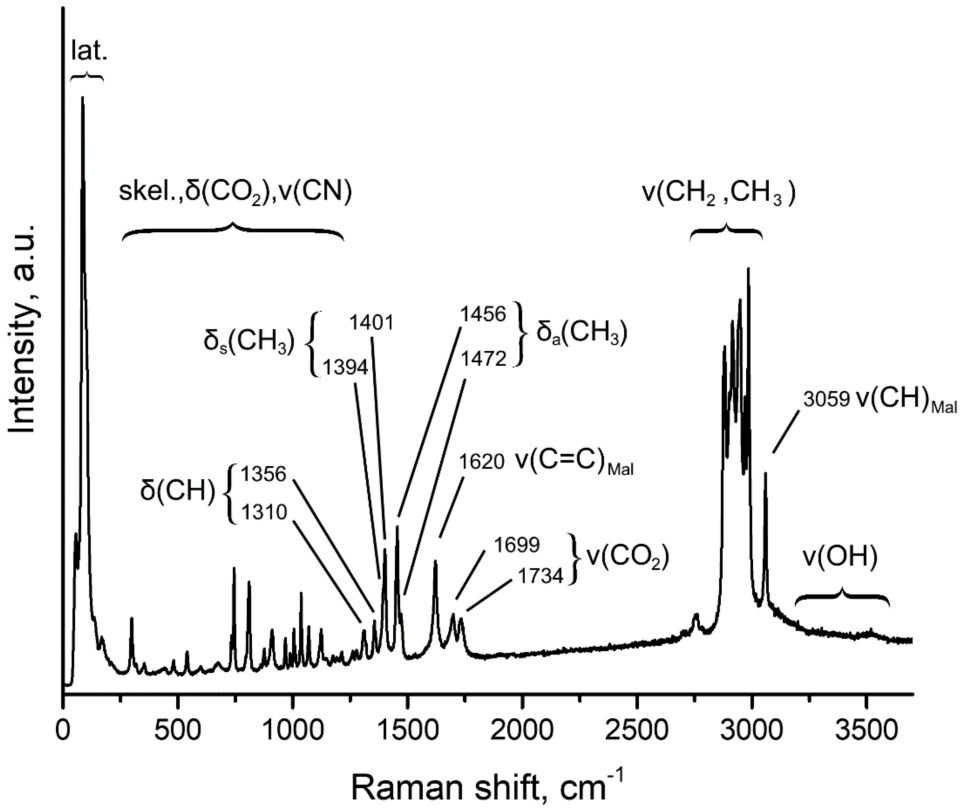

Figure 3. Experimental Raman spectra bands assignment in LLHM crystal structure at 298 K. Calculated gas-phase vibrational spectra are presented in Figure S1 (please see Supplementary Materials).

Main changes are expected in the region before 200 cm^{-1} (lattice vibrations) and 3000–3400 cm^{-1} (valence –OH and $–NH_3$ vibrations). A significant change in mode position or appearance of new modes is key evidence of phase transition, while slight changes

in peak positions or their intensities are traditional for low temperature or high-pressure behavior of the original phase.

3.2. Low Temperature Study

Low temperature Raman spectra of LLHM crystal were recorded in the temperature range of 300–11 K, cooling down the sample. No additional peaks of a new phase were found in spectra (Figure 4). No crystal changes were also found using optical microscopy on cooling.

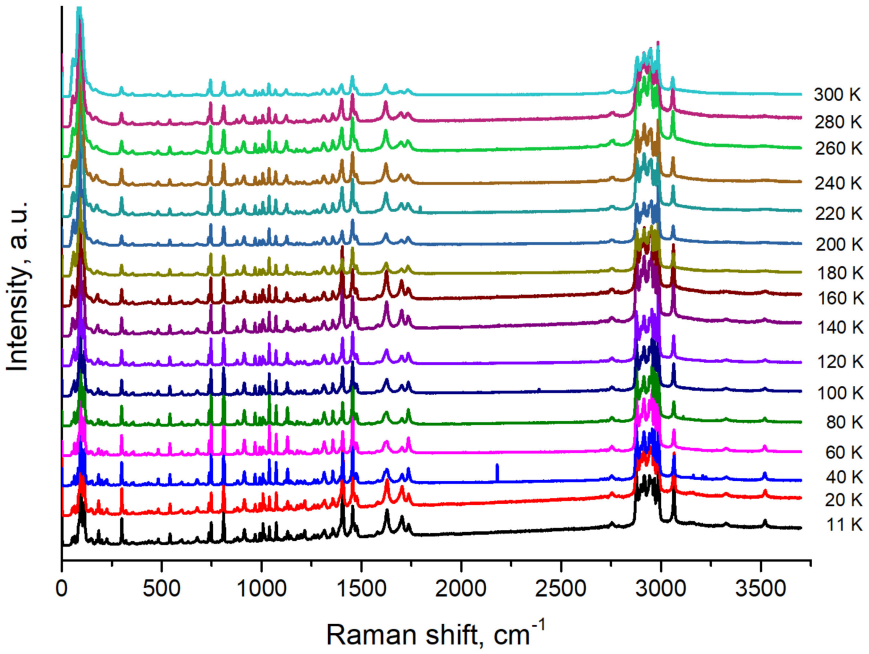

Figure 4. LLHM Raman spectra at low temperatures, showing no phase transition on cooling. Lone spurious peaks in the region of 2000–2500 cm^{-1} at temperatures 40 and 100 K were not vanished from spectra to preserve original data. Same is true for spurious peaks at 40 K in the region between 3100–3250 cm^{-1}.

Wide bands split on cooling due to the thermal motion decrease. At low temperatures, the motions of functional groups in the molecule (e.g., different CH_3 groups motion in L-Leucine ion) become distinguishable in Raman spectra. Moreover, vibrations of the same groups in symmetry unequal molecules are close in spectra, but they have slightly different frequencies (2–10 cm^{-1}) because of the crystalline environment and become distinguishable at low temperatures as well. This is a typical behavior of molecular crystals, especially with a high Z' number [68–70]. Low and high-frequency regions are shown in detail in Figure S2. Stretching vibration of CO_2^- group (1699 cm^{-1} and 1734 cm^{-1} at 298 K, see Figure 3) has a different intensity ratio, which changes at 160 K and 80 K, and may be evidence of a phase transition, e.g., a doubling of the unit cell. Nevertheless, we assume change of this vibration intensity is the result of structure shrinking and corresponding intermolecular interaction changes, but not phase transition. SCXRD in ref. [34] showed no phase transition at 160 K or at the 0–200 cm^{-1} region in Raman spectra. Based on scrupulous analysis of Raman spectra at low temperatures, one can suggest no phase transition on cooling. This coincides well with our previous X-Ray study in the temperature range of 100–300 K [34]. Summing up these two experiments, LLHM plasticity preservation can be proposed below 77 K down to liquid helium temperatures.

3.3. High Pressure Study

High pressure experiments were provided in different PTMs using DAC as reported in the Section 2. Usage of SCXRD was limited due to the poor diffraction data, which is a result

of the nature of the LLHM crystal structure (defining plasticity) and DAC construction. Thus, only Raman spectra were recorded for all high-pressure experiments.

Surprisingly, the behavior of LLHM crystals differs significantly in paraffin and PIP. An effect of PTM, as well as experiment protocol on molecular crystals phase transition at high pressure, is a documented phenomenon [43,71,72]. The low-frequency region in Raman spectra shows no phase transition in paraffin up to 2.9 GPa (close to pressure limit for paraffin) and some changes in LLHM crystal in PIP at 1.35 GPa (Figure 5).

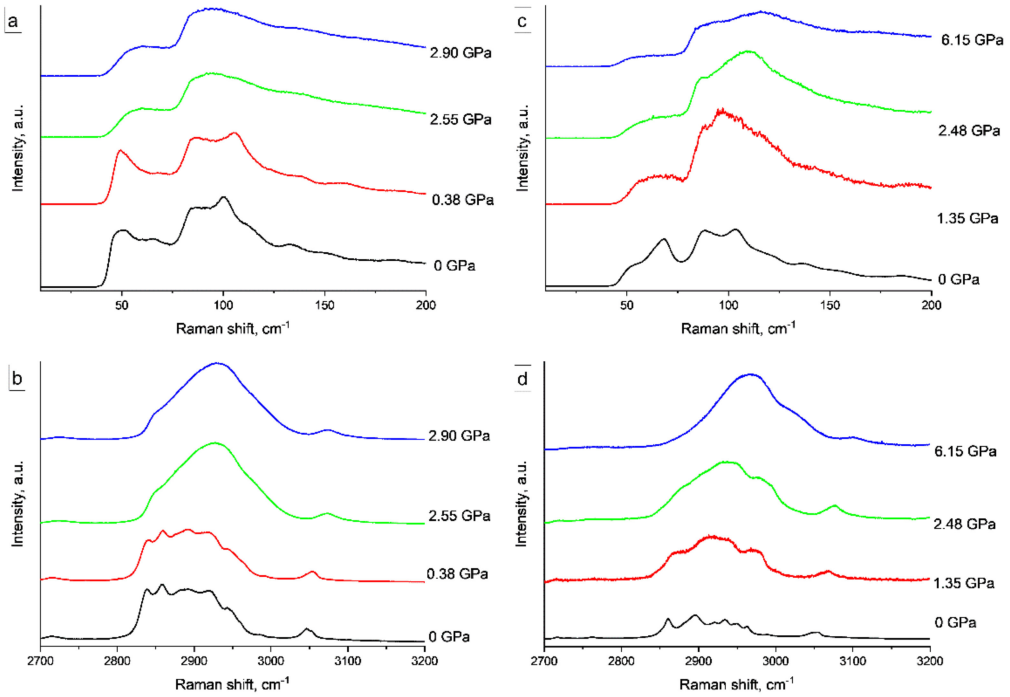

Figure 5. Raman spectra of LLHM at multiple pressures at (**a**,**c**) low-frequency and (**b**,**d**) high-frequency regions, showing different behavior in paraffin (**left**) and PIP (**right**) PTM.

The high-frequency Raman region is not very informative, lacking -OH and -NH_3 vibrational modes information at high pressures [73,74]. Nevertheless, some changes in -CH_x vibration modes confirm crystal changes in PIP in contrast to paraffin (full Raman spectra at all pressures are shown in Figure S3). We also report spectra of LLHM crystal in PIP at 0 GPa before pressure impact and after relaxation from 6.15 Gpa (Figure 6). Significant background level (halo) may be explained with possible amorphization of plastic LLHM crystal at high pressure or luminescence, which was not observed before pressure impact.

Possible phase transition in PIP was additionally confirmed by optical microscopy, which recorded crystal destruction at 1.35 GPa (Figure 7). No obvious changes of LLHM crystal in paraffin occurred in the whole pressure range according to optical microscopy. This confirms different behavior of LLHM crystals under pressure in different media.

An absence of SCXRD did not allow for the report of phase transition in LLHM crystal at high pressure in PIP unequivocally. Nevertheless, relevant changes in optical microscopy and Raman spectra allowed us to speculate about crystal destruction because of one or a cascade of phase transitions in the crystal structure or amorphization of the LLHM sample.

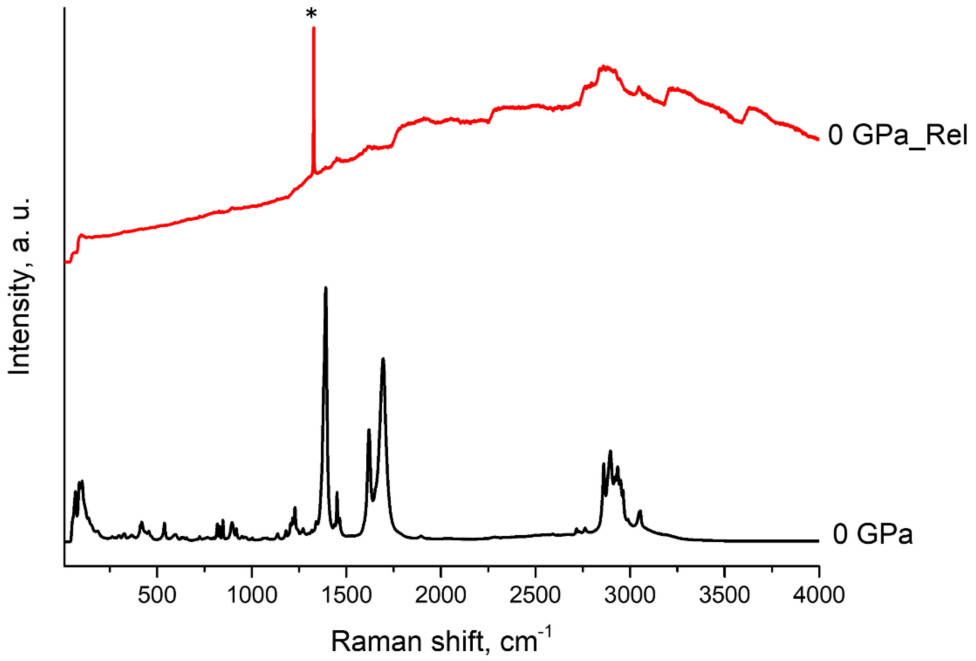

Figure 6. Raman spectra of LLHM at PIP PTM at 0 GPa before (bottom black line) and after (upper red line) pressure impact. * Asterisk mark the signal from DAC.

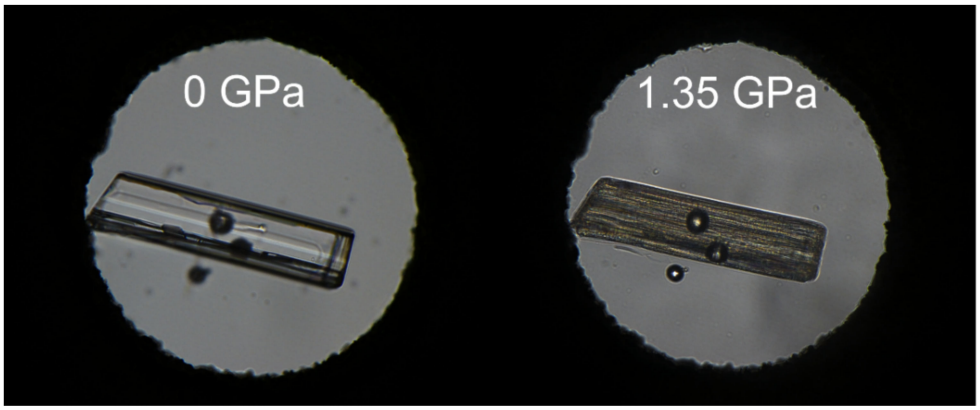

Figure 7. Photographs showing LLHM crystal destruction in PIP at pressure 1.35 GPa. LLHM crystal at 0 GPa (**left**) and 1.35 GPa (**right**). Crystal size is 0.3 mm × 0.05 mm × 0.02 mm.

4. Discussion

A search of new phases of molecular crystals at extreme conditions is an important area of modern chemistry. In this work, a unique bending crystal of LLHM, which preserves its plasticity at 77 K, was studied at low temperatures and high pressure. Based on literature data and computational vibrational spectra, major band regions were assigned to follow their changes at extreme conditions. Raman spectra of LLHM were recorded down to 11 K, showing no phase transition. Based on this experimental fact, we suggest the possibility to preserve LLHM plasticity below liquid nitrogen temperature. High pressure experiments showed different behavior of LLHM crystal in paraffin and PIP used as PTM. We found no phase transition using paraffin up to 2.95 GPa. Raman spectra and optical microscopy gave reasons to postulate the LLHM phase transition, phase transition cascade, or amorphization at high pressure, which results in crystal destruction at PIP PTM at 1.35 GPa. Additional XRPD or SCXRD using synchrotron radiation may be applied to highlight additional details of LLHM high pressure behavior in future studies.

Supplementary Materials: The following are available online at https://www.mdpi.com/article/10.3390/cryst11121575/s1, Figure S1: Gas phase calculated (a) Raman and (b) IR spectra of L-Leucine (Black), Maleic acid (Red), and L-Leucinium hydrogen maleate (Blue), Figure S2: Experimental LLHM Raman spectra at low temperatures, showing no phase transition on cooling. Detailed three different regions of Raman spectra, Figure S3: Raman spectra of LLHM at multiple pressures in PIP (left) and paraffin (right) PTM. Diamond peak from anvil cell is marked with *.

Author Contributions: Conceptualization, D.A.R.; methodology, D.A.R.; validation, D.A.R. and K.D.S.; formal analysis, K.D.S.; investigation, D.A.R.; resources, D.A.R.; data curation, D.A.R. and K.D.S.; writing—original draft preparation, D.A.R.; writing—review and editing, D.A.R.; visualization, K.D.S.; supervision, D.A.R.; project administration, D.A.R.; funding acquisition, D.A.R. All authors have read and agreed to the published version of the manuscript.

Funding: Computational part of this research was funded by the Russian Science Foundation, grant number 21-73-00094.

Data Availability Statement: The data presented in this study are available in the Supplementary Information section.

Acknowledgments: Denis Rychkov acknowledge Elena Boldyreva for basic idea to study the crystals of amino acids and their salts, including L-Leucinium Hydrogen Maleate system, at low temperatures and high pressures. All the experiments were performed at REC-008 "Molecular design and ecologically safe technologies" of the Novosibirsk State University using its instruments: The crystals of L-Leucinium Hydrogen Maleate were grown by T. Nguyen (under joint guidance of S. Arkhipov and D. Rychkov), S. Arkhipov has collected and preliminary processed Raman spectroscopy data at low temperature. E. Losev performed high-pressure X-ray diffraction and Raman spectroscopy experiments and provided the optical microphotographs. S. Arkhipov and E. Losev have performed preliminary data analysis. The authors thank S. Arkhipov and E. Losev for fruitful discussions. The authors are also grateful to A. A. Iurchenkova for assistance in preparing figures. The Siberian Branch of the Russian Academy of Sciences (SB RAS) Siberian Supercomputer Center is gratefully acknowledged for providing supercomputer facilities. The authors also acknowledge the Supercomputing Center of the Novosibirsk State University (http://nusc.nsu.ru) for providing computational resources.

Conflicts of Interest: The authors declare no conflict of interest. The funders had no role in the design of the study; in the collection, analyses, or interpretation of data; in the writing of the manuscript, or in the decision to publish the results.

References

1. Montis, R.; Fusaro, L.; Falqui, A.; Hursthouse, M.B.; Tumanov, N.; Coles, S.J.; Threlfall, T.L.; Horton, P.N.; Sougrat, R.; Lafontaine, A.; et al. Complex structures arising from the self-assembly of a simple organic salt. *Nature* **2021**, *590*, 275–278. [CrossRef] [PubMed]
2. Sobczak, S.; Ratajczyk, P.; Katrusiak, A. High-pressure Nucleation of Low-Density Polymorphs. *Chemistry* **2021**, *27*, 7069–7073. [CrossRef] [PubMed]
3. Rychkov, D.A.; Stare, J.; Boldyreva, E.V. Pressure-driven phase transition mechanisms revealed by quantum chemistry: L-serine polymorphs. *Phys. Chem. Chem. Phys.* **2017**, *19*, 6671–6676. [CrossRef] [PubMed]
4. Ghosh, S.; Mondal, A.; Kiran, M.S.R.N.; Ramamurty, U.; Reddy, C.M. The Role of Weak Interactions in the Phase Transition and Distinct Mechanical Behavior of Two Structurally Similar Caffeine Co-Crystal Polymorphs Studied by Nanoindentation. *Cryst. Growth Des.* **2013**, *13*, 4435–4441. [CrossRef]
5. Korabel'nikov, D.V.; Zhuravlev, Y.N. Semi-empirical and ab initio calculations for crystals under pressure at fixed temperatures: The case of guanidinium perchlorate. *RSC Adv.* **2020**, *10*, 42204–42211. [CrossRef]
6. Fedorov, A.Y.; Rychkov, D.A. Comparison of Different Computational Approaches for Unveiling the High-Pressure Behavior of Organic Crystals at a Molecular Level. Case Study of Tolazamide Polymorphs. *J. Struct. Chem.* **2020**, *61*, 1356–1366. [CrossRef]
7. Rychkov, D.A. A Short Review of Current Computational Concepts for High-Pressure Phase Transition Studies in Molecular Crystals. *Crystals* **2020**, *10*, 81. [CrossRef]
8. Errandonea, D. Pressure-Induced Phase Transformations. *Crystals* **2020**, *10*, 595. [CrossRef]
9. Casati, N.; Macchi, P.; Sironi, A. Molecular Crystals Under High Pressure: Theoretical and Experimental Investigations of the Solid-Solid Phase Transitions in $[Co_2(CO)_6(XPh_3)_2]$ (X=P, As). *Chemistry* **2009**, *15*, 4446–4457. [CrossRef]
10. Zakharov, B.A.; Boldyreva, E.V. High pressure: A complementary tool for probing solid-state processes. *CrystEngComm* **2019**, *21*, 10–22. [CrossRef]

11. Mazurek, A.H.; Szeleszczuk, Ł.; Pisklak, D.M. Periodic DFT Calculations—Review of Applications in the Pharmaceutical Sciences. *Pharmaceutics* **2020**, *12*, 415. [CrossRef]
12. McGregor, L.; Rychkov, D.A.; Coster, P.L.; Day, S.; Drebushchak, V.A.; Achkasov, A.F.; Nichol, G.S.; Pulham, C.R.; Boldyreva, E.V. A new polymorph of metacetamol. *CrystEngComm* **2015**, *17*, 6183–6192. [CrossRef]
13. Bauer, J.; Spanton, S.; Henry, R.; Quick, J.; Dziki, W.; Porter, W.; Morris, J. Ritonavir: An extraordinary example of conformational polymorphism. *Pharm. Res.* **2001**, *18*, 859–866. [CrossRef]
14. Zhang, G. Phase transformation considerations during process development and manufacture of solid oral dosage forms. *Adv. Drug Deliv. Rev.* **2004**, *56*, 371–390. [CrossRef]
15. Llinàs, A.; Goodman, J.M. Polymorph control: Past, present and future. *Drug Discov. Today* **2008**, *13*, 198–210. [CrossRef]
16. Chen, Y.; Chen, C.; Rehman, H.U.; Zheng, X.; Li, H.; Liu, H.; Hedenqvist, M.S. Shape-Memory Polymeric Artificial Muscles: Mechanisms, Applications and Challenges. *Molecules* **2020**, *25*, 4246. [CrossRef]
17. Liu, H.; Lu, Z.; Tang, B.; Qu, C.; Zhang, Z.; Zhang, H. A Flexible Organic Single Crystal with Plastic-Twisting and Elastic-Bending Capabilities and Polarization-Rotation Function. *Angew. Chem. Int. Ed.* **2020**, *59*, 12944–12950. [CrossRef]
18. Liu, H.; Bian, Z.; Cheng, Q.; Lan, L.; Wang, Y.; Zhang, H. Controllably realizing elastic/plastic bending based on a room-temperature phosphorescent waveguiding organic crystal. *Chem. Sci.* **2019**, *10*, 227–232. [CrossRef]
19. Ghosh, S.; Reddy, C.M. Elastic and Bendable Caffeine Cocrystals: Implications for the Design of Flexible Organic Materials. *Angew. Chem. Int. Ed.* **2012**, *51*, 10319–10323. [CrossRef]
20. Gupta, P.; Karothu, D.P.; Ahmed, E.; Naumov, P.; Nath, N.K. Thermally Twistable, Photobendable, Elastically Deformable, and Self-Healable Soft Crystals. *Angew. Chem. Int. Ed.* **2018**, *57*, 8498–8502. [CrossRef]
21. Commins, P.; Desta, I.T.; Karothu, D.P.; Panda, M.K.; Naumov, P. Crystals on the move: Mechanical effects in dynamic solids. *Chem. Commun.* **2016**, *52*, 13941–13954. [CrossRef]
22. Kakkar, S.; Bhattacharya, B.; Reddy, C.M.; Ghosh, S. Tuning mechanical behaviour by controlling the structure of a series of theophylline co-crystals. *CrystEngComm* **2018**, *20*, 1101–1109. [CrossRef]
23. Colmenero, F. Mechanical properties of anhydrous oxalic acid and oxalic acid dihydrate. *Phys. Chem. Chem. Phys.* **2019**, *21*, 2673–2690. [CrossRef]
24. Mishra, M.K.; Mishra, K.; Narayan, A.; Reddy, C.M.; Vangala, V.R. Structural Basis for Mechanical Anisotropy in Polymorphs of a Caffeine–Glutaric Acid Cocrystal. *Cryst. Growth Des.* **2020**, *20*, 6306–6315. [CrossRef]
25. Bhattacharya, B.; Roy, D.; Dey, S.; Puthuvakkal, A.; Bhunia, S.; Mondal, S.; Chowdhury, R.; Bhattacharya, M.; Mandal, M.; Manoj, K.; et al. Mechanical-Bending-Induced Fluorescence Enhancement in Plastically Flexible Crystals of a GFP Chromophore Analogue. *Angew. Chem.* **2020**, *132*, 20050–20055. [CrossRef]
26. Colmenero, F. Negative linear compressibility in nanoporous metal–organic frameworks rationalized by the empty channel structural mechanism. *Phys. Chem. Chem. Phys.* **2021**, *23*, 8508–8524. [CrossRef]
27. Masunov, A.E.; Wiratmo, M.; Dyakov, A.A.; Matveychuk, Y.V.; Bartashevich, E.V. Virtual Tensile Test for Brittle, Plastic, and Elastic Polymorphs of 4-Bromophenyl 4-Bromobenzoate. *Cryst. Growth Des.* **2020**, *20*, 6093–6100. [CrossRef]
28. Thomas, S.P.; Shi, M.W.; Koutsantonis, G.A.; Jayatilaka, D.; Edwards, A.J.; Spackman, M.A. The Elusive Structural Origin of Plastic Bending in Dimethyl Sulfone Crystals with Quasi-Isotropic Crystal Packing. *Angew. Chem. Int. Ed.* **2017**, *56*, 8468–8472. [CrossRef]
29. Reddy, C.M.; Gundakaram, R.C.; Basavoju, S.; Kirchner, M.T.; Padmanabhan, K.A.; Desiraju, G.R. Structural basis for bending of organic crystals. *Chem. Commun.* **2005**, *1*, 3945. [CrossRef]
30. Reddy, C.M.; Padmanabhan, K.A.; Desiraju, G.R. Structure−Property Correlations in Bending and Brittle Organic Crystals. *Cryst. Growth Des.* **2006**, *6*, 2720–2731. [CrossRef]
31. Worthy, A.; Grosjean, A.; Pfrunder, M.C.; Xu, Y.; Yan, C.; Edwards, G.; Clegg, J.K.; McMurtrie, J.C. Atomic resolution of structural changes in elastic crystals of copper(II) acetylacetonate. *Nat. Chem.* **2017**, *10*, 65–69. [CrossRef] [PubMed]
32. Bag, P.P.; Chen, M.; Sun, C.C.; Reddy, C.M. Direct correlation among crystal structure, mechanical behaviour and tabletability in a trimorphic molecular compound. *CrystEngComm* **2012**, *14*, 3865. [CrossRef]
33. Colmenero, F. Organic acids under pressure: Elastic properties, negative mechanical phenomena and pressure induced phase transitions in the lactic, maleic, succinic and citric acids. *Mater. Adv.* **2020**, *1*, 1399–1426. [CrossRef]
34. Arkhipov, S.G.; Losev, E.A.; Nguyen, T.T.; Rychkov, D.A.; Boldyreva, E.V. A large anisotropic plasticity of L-leucinium hydrogen maleate preserved at cryogenic temperatures. *Acta Crystallogr. Sect. B Struct. Sci. Cryst. Eng. Mater.* **2019**, *75*, 143–151. [CrossRef]
35. Nguyen, T.T.; Arkhipov, S.G.; Rychkov, D.A. Simple crystallographic model for anomalous plasticity of L-Leucinium hydrogen maleate crystals. *Mater. Today Proc.* **2020**, *25*, 412–415. [CrossRef]
36. Barrio, M.; Maccaroni, E.; Rietveld, I.B.; Malpezzi, L.; Masciocchi, N.; Céolin, R.; Tamarit, J.-L. Pressure-temperature state diagram for the phase relationships between benfluorex hydrochloride forms I and II: A case of enantiotropic behavior. *J. Pharm. Sci.* **2012**, *101*, 1073–1078. [CrossRef]
37. Fabbiani, F.P.A.; Allan, D.R.; David, W.I.F.; Moggach, S.A.; Parsons, S.; Pulham, C.R. High-pressure recrystallisation—A route to new polymorphs and solvates. *CrystEngComm* **2004**, *6*, 504–511. [CrossRef]
38. Drebushchak, V.A.; McGregor, L.; Rychkov, D.A. Cooling rate "window" in the crystallization of metacetamol form II. *J. Therm. Anal. Calorim.* **2017**, *127*, 1807–1814. [CrossRef]

39. Fabbiani, F.P.A.; Pulham, C.R. High-pressure studies of pharmaceutical compounds and energetic materials. *Chem. Soc. Rev.* **2006**, *35*, 932. [CrossRef]
40. Moggach, S.A.; Marshall, W.G.; Parsons, S. High-pressure neutron diffraction study of L-serine-I and L-serine-II, and the structure of L-serine-III at 8.1 GPa. *Acta Crystallogr. Sect. B Struct. Sci.* **2006**, *62*, 815–825. [CrossRef]
41. Wood, P.A.; Francis, D.; Marshall, W.G.; Moggach, S.A.; Parsons, S.; Pidcock, E.; Rohl, A.L. A study of the high-pressure polymorphs of L-serine using ab initio structures and PIXEL calculations. *CrystEngComm* **2008**, *10*, 1154. [CrossRef]
42. Zakharov, B.A.; Kolesov, B.A.; Boldyreva, E.V. Effect of pressure on crystalline L- and DL-serine: Revisited by a combined single-crystal X-ray diffraction at a laboratory source and polarized Raman spectroscopy study. *Acta Crystallogr. Sect. B Struct. Sci.* **2012**, *68*, 275–286. [CrossRef]
43. Fisch, M.; Lanza, A.; Boldyreva, E.; Macchi, P.; Casati, N. Kinetic Control of High-Pressure Solid-State Phase Transitions: A Case Study on l-Serine. *J. Phys. Chem. C* **2015**, *119*, 18611–18617. [CrossRef]
44. Millar, D.I.A.; Oswald, I.D.H.; Francis, D.J.; Marshall, W.G.; Pulham, C.R.; Cumming, A.S. The crystal structure of β-RDX-an elusive form of an explosive revealed. *Chem. Commun.* **2009**, *5*, 562–564. [CrossRef]
45. Munday, L.B.; Chung, P.W.; Rice, B.M.; Solares, S.D. Simulations of High-Pressure Phases in RDX. *J. Phys. Chem. B* **2011**, *115*, 4378–4386. [CrossRef]
46. Hunter, S.; Sutinen, T.; Parker, S.F.; Morrison, C.A.; Williamson, D.M.; Thompson, S.; Gould, P.J.; Pulham, C.R. Experimental and DFT-D Studies of the Molecular Organic Energetic Material RDX. *J. Phys. Chem. C* **2013**, *117*, 8062–8071. [CrossRef]
47. Ma, Y.; Zhang, A.; Xue, X.; Jiang, D.; Zhu, Y.; Zhang, C. Crystal packing of impact-sensitive high-energy explosives. *Cryst. Growth Des.* **2014**, *14*, 6101–6114. [CrossRef]
48. Millar, D.I.A. *Energetic Materials at Extreme Conditions*; Springer: Berlin/Heidelberg, Germany, 2012; ISBN 9783642231315.
49. Gude, V.; Choubey, P.S.; Das, S.; Bhaktha, B.N.S.; Reddy, C.M.; Biradha, K. Elastic orange emissive single crystals of 1,3-diamino-2,4,5,6-tetrabromobenzene as flexible optical waveguides. *J. Mater. Chem. C* **2021**, *9*, 9465–9472. [CrossRef]
50. Das, S.; Mondal, A.; Reddy, C.M. Harnessing molecular rotations in plastic crystals: A holistic view for crystal engineering of adaptive soft materials. *Chem. Soc. Rev.* **2020**, *49*, 8878–8896. [CrossRef]
51. Matveychuk, Y.V.; Bartashevich, E.V.; Tsirelson, V.G. How the H-Bond Layout Determines Mechanical Properties of Crystalline Amino Acid Hydrogen Maleates. *Cryst. Growth Des.* **2018**, *18*, 3366–3375. [CrossRef]
52. Arkhipov, S.G.; Rychkov, D.A.; Pugachev, A.M.; Boldyreva, E.V. New hydrophobic L-amino acid salts: Maleates of L-leucine, L-isoleucine and L-norvaline. *Acta Crystallogr. Sect. C Struct. Chem.* **2015**, *71*, 584–592. [CrossRef] [PubMed]
53. Rychkov, D.A.; Arkhipov, S.G.; Boldyreva, E.V. Simple and efficient modifications of well known techniques for reliable growth of high-quality crystals of small bioorganic molecules. *J. Appl. Crystallogr.* **2014**, *47*, 1435–1442. [CrossRef]
54. Boehler, R. New diamond cell for single-crystal x-ray diffraction. *Rev. Sci. Instrum.* **2006**, *77*, 115103. [CrossRef]
55. Piermarini, G.J.; Block, S.; Barnett, J.D. Hydrostatic limits in liquids and solids to 100 kbar. *J. Appl. Phys.* **1973**, *44*, 5377–5382. [CrossRef]
56. Zakharov, B.A.; Achkasov, A.F. A compact device for loading diamond anvil cells with low-boiling pressure-transmitting media. *J. Appl. Crystallogr.* **2013**, *46*, 267–269. [CrossRef]
57. Piermarini, G.J.; Block, S.; Barnett, J.D.; Forman, R.A. Calibration of the pressure dependence of the R1 ruby fluorescence line to 195 kbar. *J. Appl. Phys.* **1975**, *46*, 2774–2780. [CrossRef]
58. Forman, R.A.; Piermarini, G.J.; Barnett, J.D.; Block, S. Pressure Measurement Made by the Utilization of Ruby Sharp-Line Luminescence. *Science* **1972**, *176*, 284–285. [CrossRef]
59. Frisch, M.J.; Trucks, G.W.; Schlegel, H.B.; Scuseria, G.E.; Robb, M.A.; Cheeseman, J.R.; Scalmani, G.; Barone, V.; Mennucci, B.; Petersson, G.A.; et al. GAUSSIAN 09. Revision D.01. Gaussian Inc.: Wallingford, CT, USA, 2016.
60. Mirone, P.; Chiorboli, P. Infrared and Raman spectra and vibrational assignment of maleic anhydride. *Spectrochim. Acta* **1962**, *18*, 1425–1432.
61. Shakhse Emampour, J.; Suh, J.S.; Moskovits, M. Raman Study of the Photochemistry of Maleic Acid Adsorbed on the Surface of Colloidal Silver. *Iran. J. Chem. Chem. Eng.* **1994**, *13*, 30–36.
62. Façanha Filho, P.F.; Freire, P.T.C.; Lima, K.C.V.; Mendes Filho, J.; Melo, F.E.A.; Pizani, P.S. Raman spectra of L-leucine crystals. *Brazilian J. Phys.* **2007**, *38*, 12.
63. Façanha Filho, P.F.; Freire, P.T.C.; Lima, K.C.V.; Mendes Filho, J.; Melo, F.E.A.; Pizani, P.S. High temperature raman spectra of L-leucine crystals. *Brazilian J. Phys.* **2008**, *38*, 131–137. [CrossRef]
64. Zhu, G.; Zhu, X.; Fan, Q.; Wan, X. Raman spectra of amino acids and their aqueous solutions. *Spectrochim. Acta Part A Mol. Biomol. Spectrosc.* **2011**, *78*, 1187–1195. [CrossRef]
65. Bellamy, L.J. *The Infrared Spectra of Complex Molecules*, 2nd ed.; Springer: Dordrecht, The Netherlands, 1980; Volume 2, ISBN 9789401165228.
66. Socrates, G. Infrared Characteristic Group Frequencies. Tables and Charts. *Anal. Chim. Acta* **1994**, *296*, 221–222.
67. Hemalatha, A.; Arulmani, S.; Sanjay, P.; Deepa, K.; Madhavan, J.; Senthil, S. Growth and Characterization of L-Leucenium Hydrogen Maleate Single Crystals for Nonlinear Optical Applications. *IOP Conf. Ser. Mater. Sci. Eng.* **2018**, *360*, 012044. [CrossRef]
68. Galkina, Y.A.; Vershinin, M.A.; Kolesov, B.A. Raman Spectra of Molecular Crystals with Strong Hydrogen Bonds N-H···N in the Temperature Range of 5–300 K. *J. Struct. Chem.* **2019**, *60*, 398–404. [CrossRef]
69. Kolesov, B.A. IR and Raman spectra of strong OHO hydrogen bonds. *J. Mol. Struct.* **2021**, *1233*, 130093. [CrossRef]

70. Kolesov, B. Hydrogen Bonds: Raman Spectroscopic Study. *Int. J. Mol. Sci.* **2021**, *22*, 5380. [CrossRef]
71. Zakharov, B.A.; Tumanov, N.A.; Boldyreva, E.V. β-Alanine under pressure: Towards understanding the nature of phase transitions. *CrystEngComm* **2015**, *17*, 2074–2079. [CrossRef]
72. Anis, B.; Börrnert, F.; Rümmeli, M.H.; Kuntscher, C.A. Role of the pressure transmitting medium on the pressure effects in DWCNTs. *Phys. Status Solidi* **2013**, *250*, 2616–2621. [CrossRef]
73. Gaydamaka, A.A.; Arkhipov, S.G.; Zakharov, B.A.; Seryotkin, Y.V.; Boldyreva, E.V. Effect of pressure on slit channels in guanine sodium salt hydrate: A link to nucleobase intermolecular interactions. *CrystEngComm* **2019**, *21*, 4484–4492. [CrossRef]
74. Yang, S.Y.; Butler, I.S. Pressure-tuning infrared and Raman microscopy study of the DNA bases: Adenine, guanine, cytosine, and thymine. *J. Biomol. Struct. Dyn.* **2013**, *31*, 1490–1496. [CrossRef]